Hindawi
Advances in Materials Science and Engineering
Volume 2020, Article ID 2130341, 10 pages
https://doi.org/10.1155/2020/2130341

Research Article

Influence of Bionic Pit Structure on Friction and Sealing Performance of Reciprocating Plunger

Tianyu Gao,[1,2] Bo Su,[3] Lei Jiang,[3] and Qian Cong [1,2]

[1]*Key Laboratory of Bionic Engineering, Ministry of Education, Jilin University, Changchun, China*
[2]*State Key Laboratory of Automotive Simulation and Control, Jilin University, Changchun, China*
[3]*China North Vehicle Research Institute, Beijing, China*

Correspondence should be addressed to Qian Cong; congqian@jlu.edu.cn

Received 1 April 2020; Revised 10 June 2020; Accepted 26 June 2020; Published 16 July 2020

Academic Editor: Antonio Boccaccio

A new kind of pit-shaped bionic plunger proposes to reduce the frictional resistance of the reciprocating plunger and improve its sealing performance. According to the dorsal pore of earthworm, the bionic pit structure with different parameters designed and processed. The friction resistance test, observation test, and finite element analysis carried out. The results show that the bionic pit structure can improve the lubrication condition of the plunger surface and reduce the frictional resistance with a maximum drag reduction rate of 14.32%. The pit-shaped bionic structure can increase the storage of lubricating oil, intercept the surface streamline, and decrease the flow rate. The bionic plungers' mean contact pressure and oil film pressure increased significantly.

1. Introduction

Reciprocating moving parts are an essential indicator of a country's manufacturing level and account for a large proportion of manufacturing equipment. The plunger is a typical reciprocating moving part and is widely used in various pumping mechanisms, such as plunger pump [1–3], concrete pump [4], and drilling mud pump [5, 6]. How to reduce the frictional resistance of plunger and improve its sealing performance is a crucial issue to be solved.

Research directions for reciprocating moving parts mainly include friction, wear, lubrication, sealing, and numerical simulation [7–9]. Azzi et al. found that high friction and low sealing performance due to incorrect sealing material or geometry selection, improper surface texture, incompatible lubricants, or other frictional factors [10]. Hakami et al. and Persson studied the wear mechanism of rubber and related influence parameters and analyzed the relationship between the parameters affecting rubber wear performance and the influencing factors [11, 12]. Wu et al. applied bionic nonsmooth surface technology to high-pressure seawater pumps to explore the lubrication law of different forms of bionic pits [13]. Liu et al. studied the lubrication and sealing rules of plungers [14]. Zhang et al. explores ways to predict seal failure [15]. In order to explore the friction mechanism, Tsala et al. simulated the contact pressure, Von-Mises stress, and flow field [16–18].

In this paper, we take the plunger as the research object, and the earthworm as the bionic prototype. The influence of the bionic pit structure on the friction and sealing performance of the plunger was studied. Furthermore, we use numerical simulation methods to explore friction and sealing mechanisms. The bionic plunger proposed in this paper is of great significance for the study of plunger drag reduction and sealing technology.

2. Experiment

2.1. Design and Processing. Related studies have shown that the dorsal pores of earthworm are opened under the stimulation of alcohol and spray body fluid up to 20 cm in height [19]. There are regular pits on the surface of earthworm to secrete body fluid, which makes earthworm have a unique self-lubrication mechanism [20]. Figure 1 shows the dorsal pore of the earthworm and its excreted body fluid. When the earthworm moves through the soil, the dorsal

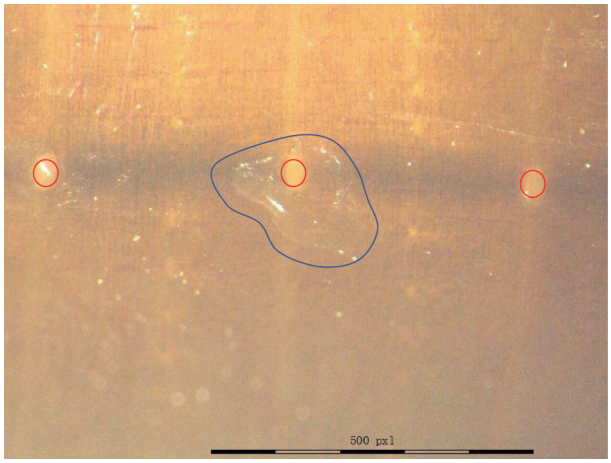

Figure 1: The dorsal pore and excreted body fluid of the earthworm.

pore will eject the body fluid secreted by the mucous membrane cells of the skin. The body fluid distributes on the earthworm's surface and permeates into the surrounding soil. The dorsal pore forms a lubricating film on the surface of the earthworm, reducing the friction resistance with the soil [21]. Through the observation of the dorsal pore, we found that is a pit structure.

Plunger pump works by connecting the steel core with the plunger, and then the steel core drives the plunger to reciprocate in the cylinder liner. In this paper, the standard plunger is a cylindrical structure with an outer diameter of $\Phi = 70$ mm and a height of $H = 30$ mm. The plungers made of rubber (elastomeric materials with nonlinear geometry and material behavior). Based on the standard plunger, the bionic pit arrays are processed onto the external surface by CYNC-400P CNC lathe produced by the Yunnan machine tool factory, as shown in Figure 2.

Pit size, density, and depth are important parameters affecting the performance of a bionic plunger. The bionic pit-shaped plunger design includes three parameters: the pit diameter d, the pit center angle α, and the pit depth h, respectively (Figure 3(b)). Figure 3(a) shows the processed bionic plungers. The pit-shaped structure on the surface of the plunger is staggered. The center spacing of the adjacent pits in the axial direction of the pit array maintains at a certain distance of 8 mm. Use L_9 (3^4) orthogonal table to prepare the experimental scheme. The structural parameters of nine groups of bionic plungers are shown in Table 1.

2.2. Friction Resistance Test. A plunger test bench is developed for friction resistance in this paper, as shown in Figure 4. The test conditions for the frictional resistance of all plungers are identical, as shown in Table 2. The liquid in the sealing chamber is water. A tensile pressure sensor measures the frictional resistance of the plunger in the upward stroke. Before the test, zero the force sensor without force, force the sensor with a standard dynamometer, and calibrate the force in the range in the software. For every 500 reciprocating movements of the plunger, calculate the mean

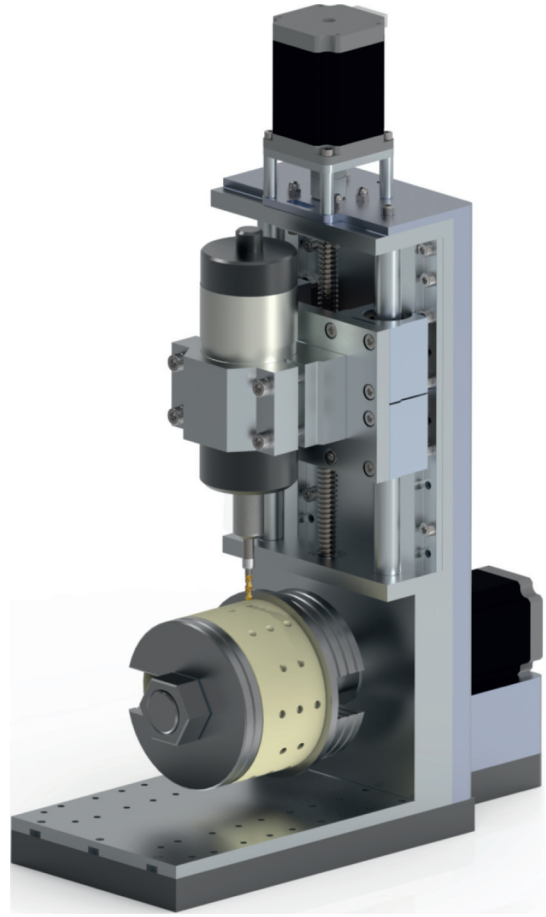

Figure 2: Machining of plungers.

value f of the friction data. The mean of the sampling data is the mean friction resistance of plunger (f), where f_1, f_2, and f_n are the sampling data values of the friction force, and n is the number of sampling points.

$$f = \frac{f_1 + f_2 + \cdots + f_n}{n}. \quad (1)$$

2.3. Observation Test. For observing the dynamic lubrication state of the plunger, replace the structural steel cylinder liner with a transparent plexiglass cylinder liner. Use Phantom v9.1 high-speed camera to observe the rapid change of lubricating oil on the plunger surface and in the pit. The plunger observation device is shown in Figure 5(a). To ensure observation stability, the high-speed camera lens and reciprocating plunger should maintain the same rate of motion. Therefore, we designed a synchronous observation test bench, whose structure shown in Figure 5(b).

3. Results and Discussion

3.1. Friction Resistance Test Result. The relationship between the friction resistance (f) and reciprocating times of the bionic plunger and the standard plunger is shown in Figure 6. In the first 2500 times of reciprocating motion, the friction of plunger increases with reciprocating times. After

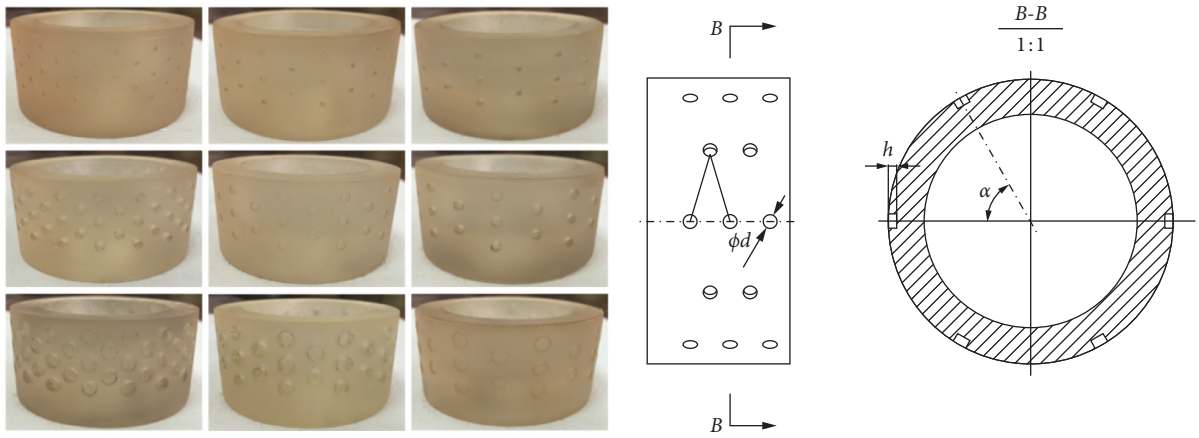

Figure 3: (a) Processed bionic plungers and (b) structure and parameters of bionic pit arrays.

Table 1: The structural parameters of bionic plungers.

Plunger number	Structural parameters		
	d (mm)	α (°)	h (mm)
1	1.5	15	1.0
2	1.5	20	2.5
3	1.5	30	4.0
4	3.0	15	4.0
5	3.0	20	1.0
6	3.0	30	2.5
7	4.5	15	2.5
8	4.5	20	4.0
9	4.5	30	1.0

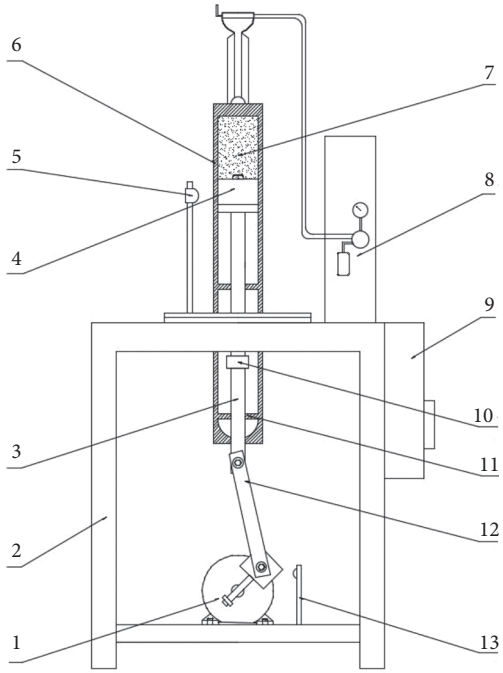

Figure 4: Test bench: 1: drive motor; 2: pedestal base; 3: pull rod; 4: plunger; 5: high-speed camera; 6: cylinder liner; 7: sealed chamber; 8: pressure control device; 9: data acquisition control box; 10: pull pressure sensor; 11: locating pin; 12: adjustable stroke crank; 13: speed sensor.

Table 2: The test conditions.

Test conditions	
Plunger stroke	30 mm
Linear velocity	25 mm/s
Load pressure	1.5 MPa
Reciprocating times	10000

the plunger reciprocated 2500 times, the friction of the plunger did not change significantly and tended to be stable. During the early cycle, the friction surface has a sufficiently thick lubricating oil layer, and the friction pair is in liquid lubrication condition with less friction resistance. As time goes on, the friction gradually changes to a stable mixed lubricating condition, which results in stable friction resistance.

The average friction value of the plunger after 2500 reciprocating motions is taken as the average friction (F) of the plunger, as shown in Figure 7. Since the pit diameter is too small, the F of No. 1, No. 2, and No. 3 plungers is almost identical to that of the standard plunger, and the drag reduction effect is not significant. Among the nine groups of bionic plungers, the No. 7 plunger had the lowest F, with a drag reduction rate of 14.32%.

The friction resistance of nine groups of the bionic plunger is less than that of the standard plunger. The reason for this phenomenon is that the pits on the plunger surface improve the lubrication conditions and reduce the frictional resistance between the plunger and the cylinder liner. Different parameters of the pit structure have different influences on the lubrication between the cylinder liner and plunger. Figure 8 shows the influence rule of different pit parameters on plunger frictional resistance. The change of d has the most considerable influence on plunger friction, while α and h have little effect on it. The storage amount of lubricating oil increases as d increases and the frictional resistance decreases simultaneously. Therefore, under the premise that plunger strength allows, the d should not be too small. When α increased, the pit density on the surface of the plunger reduced, which is not conducive to oil storage and

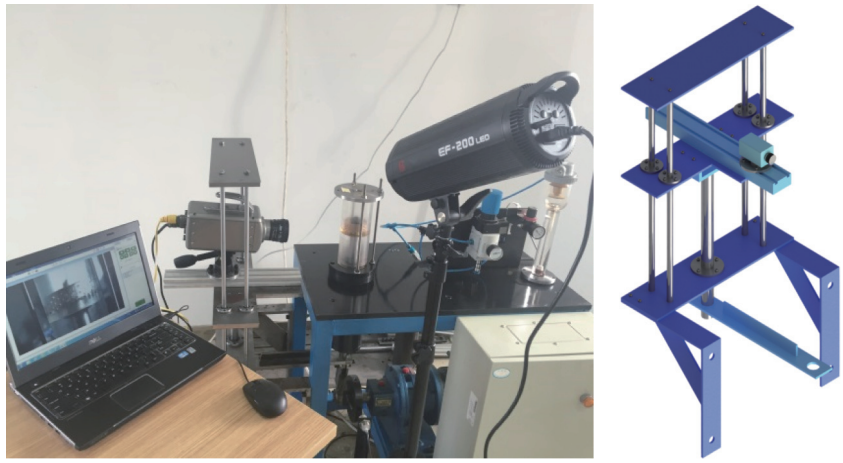

(a) (b)

Figure 5: Plunger observation device (a) and synchronous observation test bench (b).

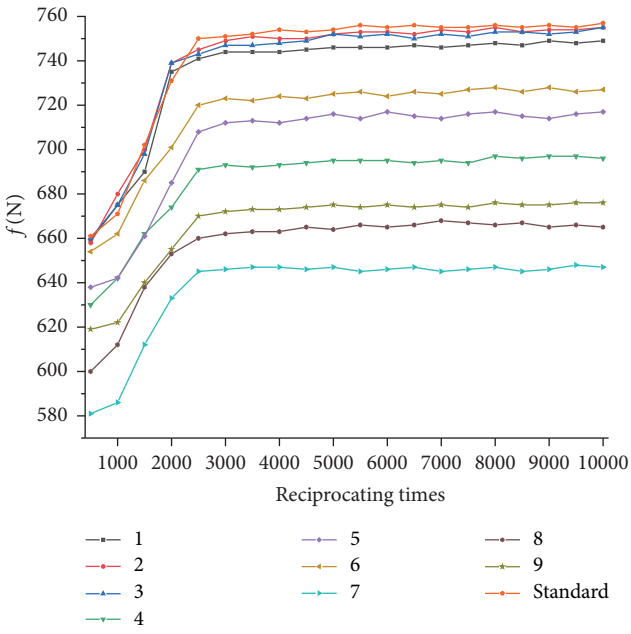

Figure 6: The relationship between f and the reciprocating times.

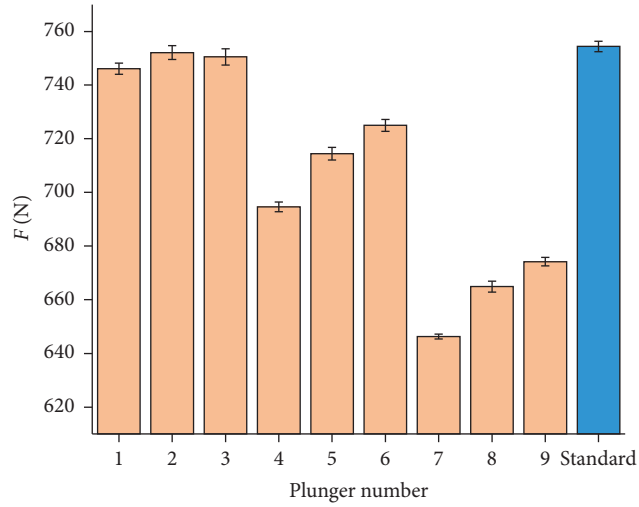

Figure 7: F of the plungers.

lubrication. The plunger friction increases with the increase of α. The oil storage capacity of the pit increases with the increase of h and simultaneously reduces the loss of lubricating oil in the reciprocating motion of the plunger.

3.2. Observation Test Result. The observation test result of the standard plunger and the bionic plunger is shown in Figure 9. The pit-shaped bionic structure can enlarge the lubrication flow field space between the plunger and the cylinder liner and increase the storage of lubricating oil. As shown in Figure 9(a), when the standard plunger reciprocates, the surface lubricating oil flows in parallel from top to bottom, and the surface of the plunger hardly hinders the lubricating oil. Therefore, the standard plunger surface lubricating oil loss faster. Figure 9(b) shows the results of the No. 1 plunger. The lubricating oil in the pit (A) has a remarkable rotation phenomenon, and there is a slight backflow of the lubricating oil around the pit (B). Both of these two phenomena can hinder the loss of lubricating oil to a certain extent, improve lubrication conditions, and reduce frictional resistance.

4. Finite Element Analysis of Plunger

To study the friction and sealing mechanism, the standard and bionic plungers analyzed by ANSYS. Plungers, cylinder liners, and steel core models created in the modeling software and assembled into the finite analysis software. The roughness of cylinder liner is 2.0 μm. The rigidity of cylinder liner and steel core is much higher than that of rubber plunger, which simplified as rigid body with elastic modulus of 210 GPa, density of 7800 kg/m^3, and Poisson's ratio of 0.3. The rubber is a typical kind of hyperelastic material, and the Mooney-Rivlin model [5, 22] is selected, in which the analytical constant C10 is 2.5 MPa, C01 is 0.625 MPa, and the

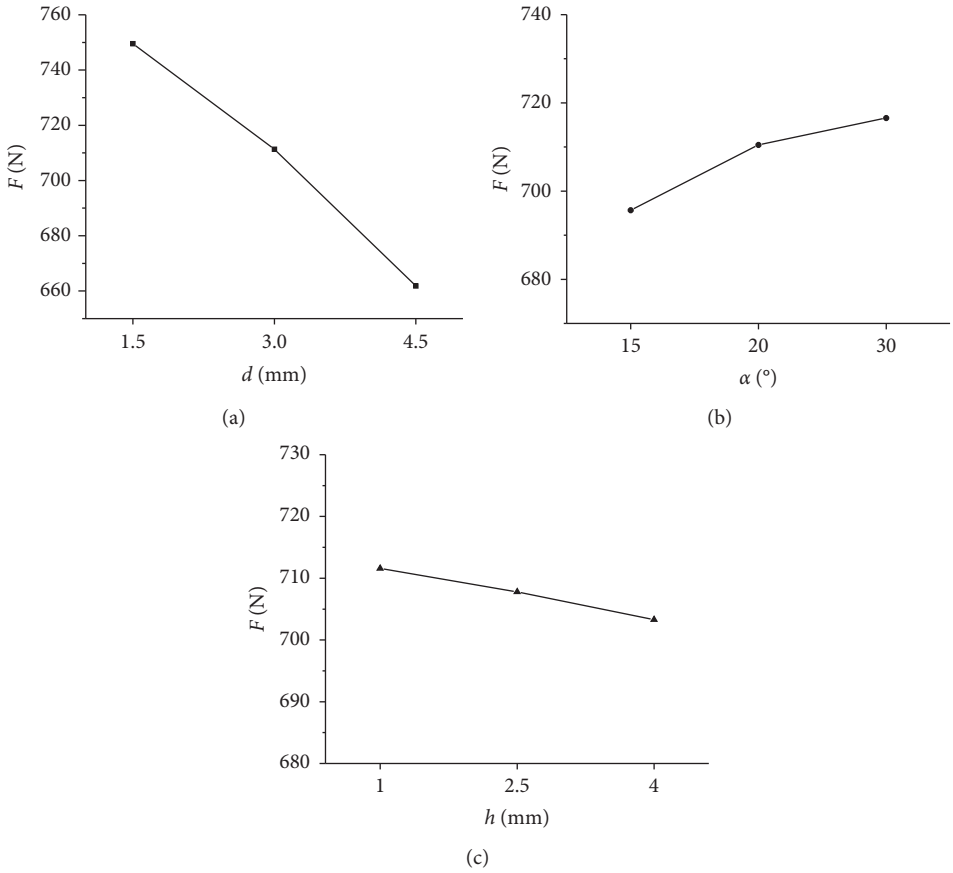

Figure 8: The influence on plunger frictional resistance: (a) d, (b) α, (c) h.

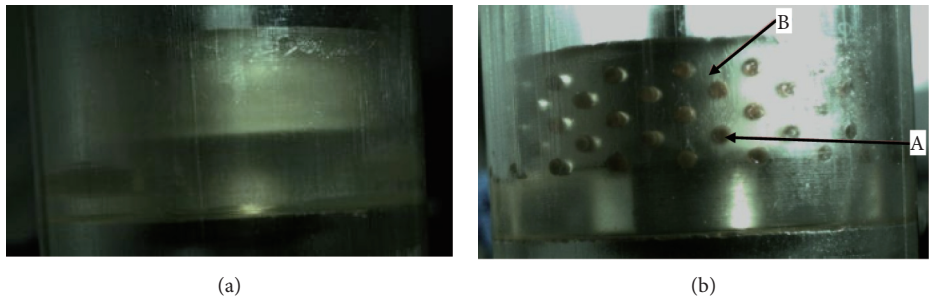

Figure 9: The observation test result. (a) Standard plunger, (b) No. 1 plunger.

density is 1120 kg/m^3. The Hex Dominant model selected for the grid division of plunger, cylinder liner, and steel core. The mesh division of contact surface between plunger and cylinder liner refined. For the accuracy of the solution, the minimum grid element controlled at 1 mm.

The cylinder liner set to fixed during the simulation. Since we selected one-half of the model, the symmetry plane set to frictionless support. We divided the analysis load into three steps, each of which set at 0.5 s. Firstly, we simulated the interference fit of the plunger in cylinder liner to make the plunger have the initial sealing effect. Then, the working pressure of 1.5 MPa was applied to the plunger's pressure surface to simulate the working condition of plunger pumping. Finally, to simulate the stroke of the plunger motion, a displacement of 30 mm was applied to the steel core. The settings of the analysis load step shown in Figure 10.

The plunger's seal failure is mainly due to the gap between the plunger and the cylinder liner. Abrasive particles participate in the contact movement between the plunger and the cylinder liner, which causes both the plunger and the cylinder liner worn. The higher the contact pressure between plunger and cylinder liner, the less likely it is for abrasive particles to enter the contact surface of the friction pair. The sealing mechanism of the bionic pit-shaped plunger is revealed by analyzing the contact pressure of the plunger sealing surface. The plunger is separately extracted from the assembly for force analysis to obtain the surface contact

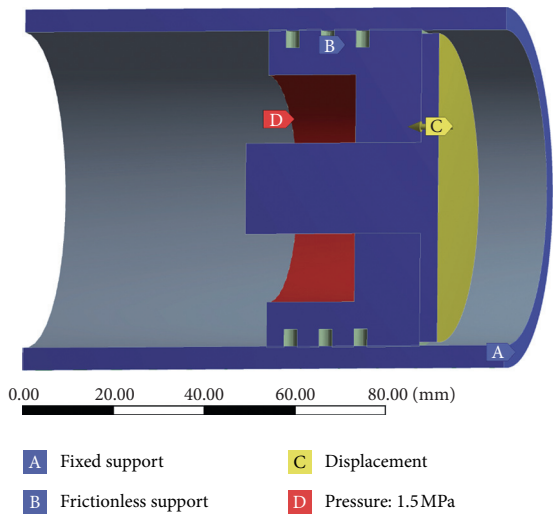

Figure 10: The settings of the analysis load step.

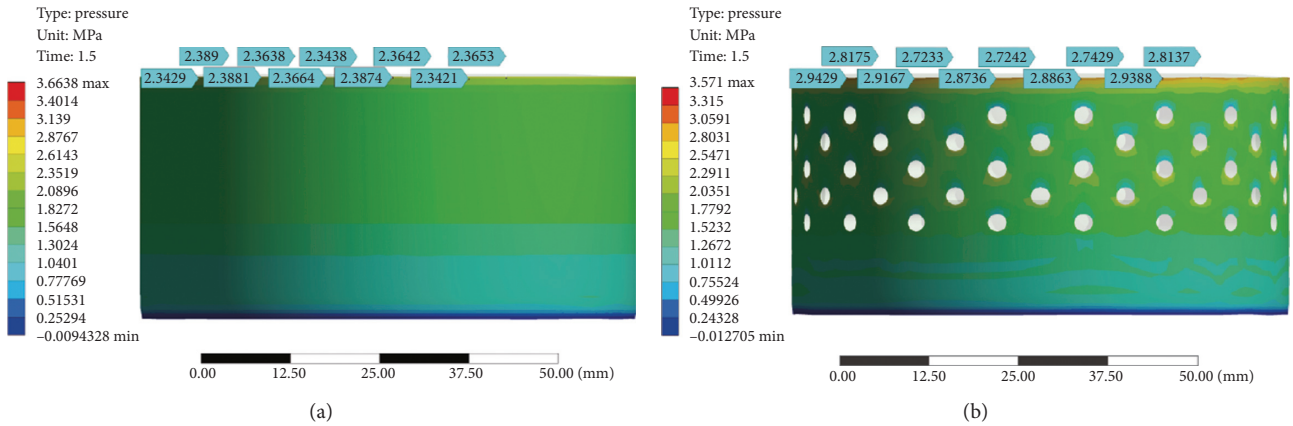

Figure 11: The nodes of plunger: (a) standard plunger, (b) No. 1 plunger.

pressure. We take ten nodes which are at equal intervals at the edge of the plunger seal to obtain the contact pressure values of the respective nodes, as shown in Figure 11.

The average of the contact pressures of the ten nodes was taken as the mean contact pressure (P), as shown in Figure 12. The P of the bionic plunger is higher than that of the standard plunger. The pit structure increases the P of the plunger sealing part, effectively preventing the abrasive particles from entering into the friction pair and increasing the sealing performance of the plunger. The P of the No. 7 bionic plunger was 2.838 MPa, which was 19.98% higher than 2.3653 MPa of the standard plunger. After 10000 reciprocating movements, the leakage of the plunger was as shown in Figure 12. Compared with the standard plunger, the leakage of bionic plungers is smaller. No. 4 and No. 7 plungers have the least leakage with high contact pressure.

The simulation analysis of lubricating oil was performed using the CFX module in the ANSYS software. The models of the lubricant fluid domain was completed by Cero software and imported into the CFX module. Set and name the inlet, outlet, and wall of the fluid domain, respectively. Mesh method is Hex Dominant Method, and Element Size is 1 mm, as shown in Figure 13. The mesh of inlet, outlet, and bionic pits refined to level 2. Then define the lubricating oil material properties in the material library: set the density to 876 kg/m^3, and set the dynamic viscosity to 680 cst. Finally, the boundary conditions set in CFX-pre. Set the pressure of the inlet lubricating oil to 1.5 MPa and the outlet pressure to 1 MPa.

The lubricating oil streamline of standard and No. 7 plunger is shown in Figure 14. No significant changes in the flow rate of the surface streamline on the standard plunger. The pits of the bionic plunger can increase the storage and decrease the loss of lubricating oil. Bionic pits intercept the surface streamline on the plunger and decrease the flow rate of the nearby streamline. Thus, the lubricating condition of the fluid domain is improved, and the friction force of the friction pair decreased.

We analyzed the oil film pressure of plungers, as shown in Figure 15. Due to the existence of the bionic pits, the plungers' oil film pressure increased significantly, and the bearing capacity of the oil film increased. The average oil film pressure (p) of plungers is shown in Figure 16. It can be seen that the average oil film pressure of No. 7 plunger is higher, resulting in better lubrication conditions and less friction.

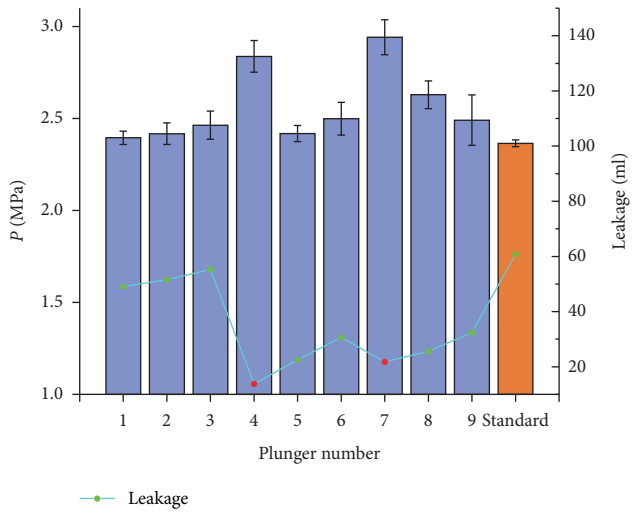

Figure 12: The mean contact pressure P.

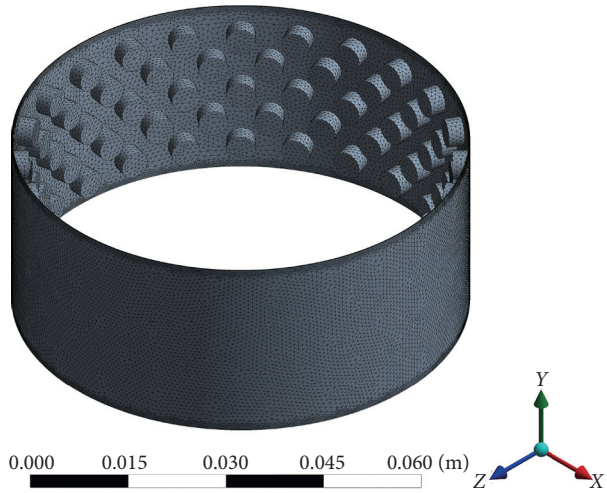

Figure 13: Mesh method and size.

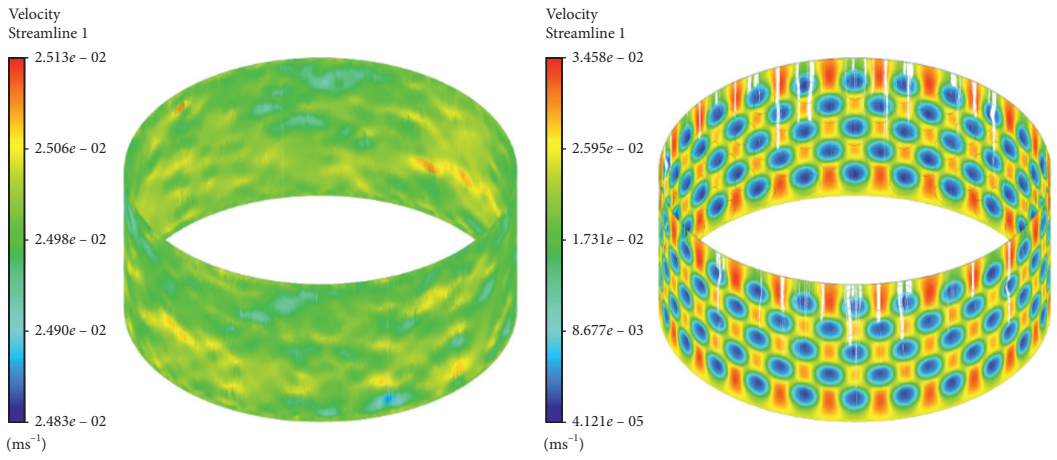

(a) (b)

Figure 14: Lubricating oil streamline: (a) standard plunger; (b) No. 7 plunger.

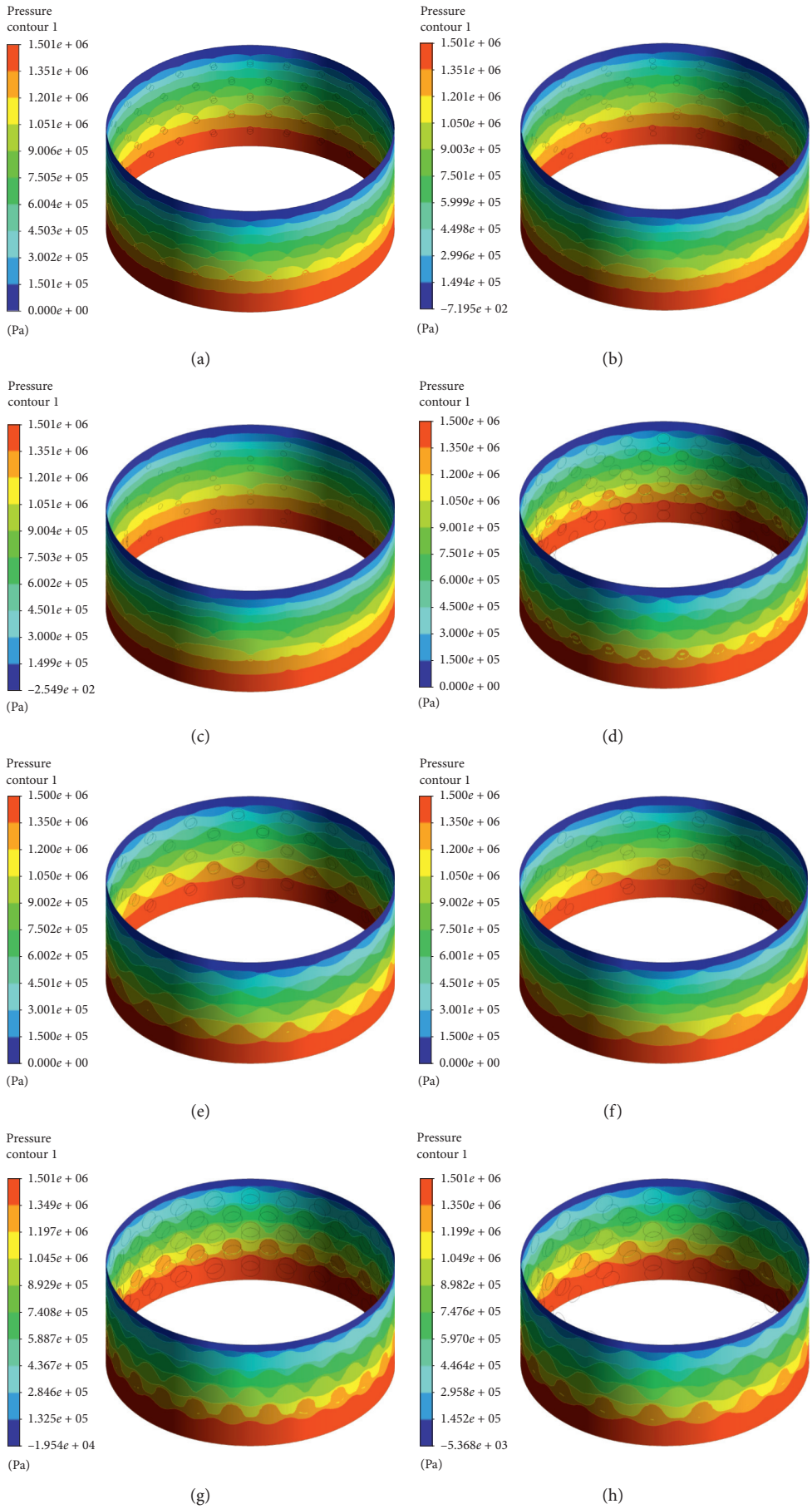

Figure 15: Continued.

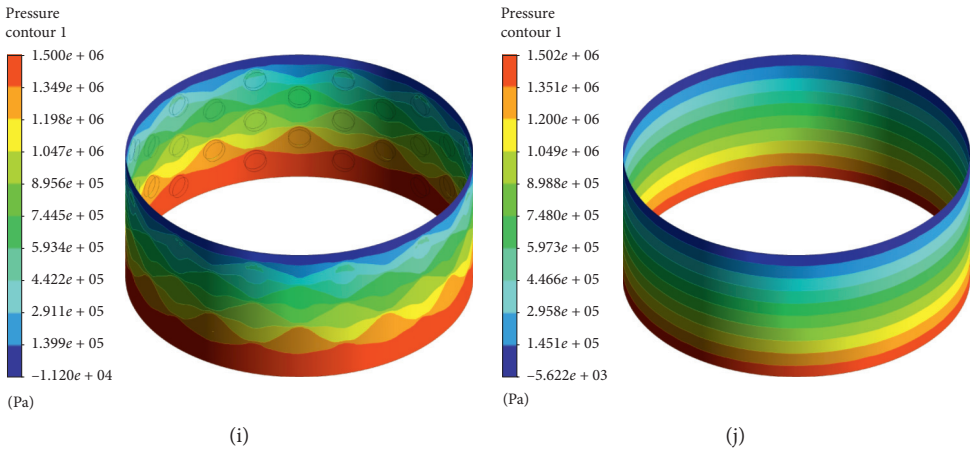

Figure 15: Oil film pressure.

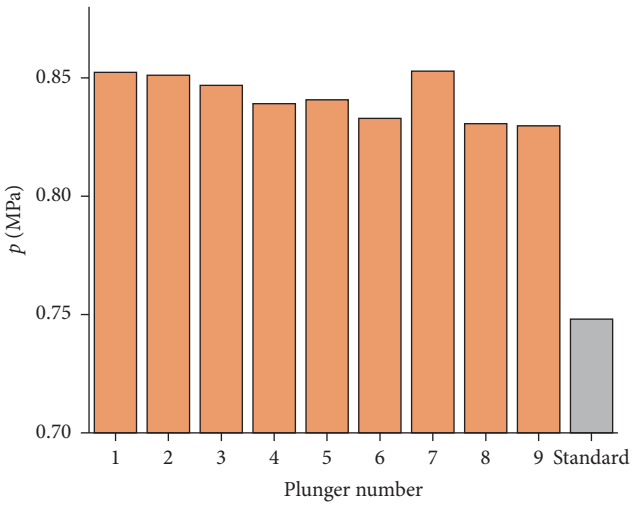

Figure 16: Average oil film pressure p.

5. Conclusion

(1) The bionic pit structure can improve the lubrication condition of the plunger surface and reduce the frictional resistance. The No. 7 plunger has a maximum drag reduction rate of 14.32%. The change of d has the most considerable influence on plunger friction.

(2) The pit-shaped bionic structure can increase the storage of lubricating oil. The remarkable rotation of lubricating oil in pits and the slight backflow around pits can hinder the loss of lubricating oil to a certain extent. Bionic pits can intercept the surface streamline and decrease the flow rate.

(3) The bionic plungers' mean contact pressure (P) is higher than that of the standard plunger. The bionic plungers' oil film pressure (p) increased significantly, and the bearing capacity of the oil film increased.

Data Availability

All data and models generated or used during the study are included in the article.

Conflicts of Interest

The authors declared no potential conflicts of interest with respect to the research, authorship, and/or publication of this article.

Acknowledgments

This study was supported by the National Key R&D Program of China (Grant No. 2017YFD0700202), the National Natural Science Foundation of China (Grant Nos. 51775234 and 91748211), and the State Key Laboratory Fund of Automobile Simulation and Control (Grant No. 20171115).

References

[1] Z. Q. Dai, T. Z. Zhang, and M. L. Wan, "The fuel consumption of the integrated piston-plunger pump," in *Resources and Sustainable Development, Pts 1–4*, J. Wu, X. Lu, H. Xu, and N. Nakagoshi, Eds., pp. 2699–2703, Trans Tech Publications Ltd, Zurich, Switzerland, 2013.

[2] K. R. Urazakov, B. M. Latypov, and B. K. Ishmukhametov, "Experimental studies of the influence of configuration of regular microrelief of plunger surface on sucker-rod pump delivery," *Chemical and Petroleum Engineering*, vol. 54, no. 3-4, pp. 172–176, 2018.

[3] X. T. Han, X. D. Li, Y. L. Wang et al., "Optimal desigh of self-sealing low friction and non-leakage plunger pump," in *Advanced Manufacturing Technology*, J. T. Han, Z. Y. Jiang, and S. Jiao, Eds., p. 1653, Trans Tech Publications Ltd, Zurich, Switzerland, 2011.

[4] Y. J. Zhan, J. Gong, Y. L. Huang, C. Shi, Z. B. Zuo, and Y. Q. Chen, "Numerical study on concrete pumping behavior via local flow simulation with discrete element method," *Materials*, vol. 12, no. 9, p. 1415, 2019.

[5] Q. Cong, T. Y. Gao, Y. W. Sun, and W. J. Tian, "Sealing performance of bionic striped mud pump piston," *Advances in Materials Science and Engineering*, vol. 2019, Article ID 8751540, 9 pages, 2019.

[6] T. Y. Gao, X. J. Wang, Y. W. Sun, X. J. Cheng, and Q. Cong, "Friction and wear performance of bionic stripped piston of BW-160 slime pump," *Proceedings of the Institution of*

Mechanical Engineers, Part C: Journal of Mechanical Engineering Science, vol. 234, no. 4, pp. 872–881, 2020.

[7] Z. Ma, Y. M. Li, and L. Z. Xu, "Experimental study of reciprocating friction between rape stalk and bionic nonsmooth surface units," *Applied Bionics and Biomechanics*, vol. 2015, Article ID 627960, 9 pages, 2015.

[8] P. Cai, Z. F. Luo, X. H. Duan, and X. S. Qin, "Effect of reciprocating and unidirectional sliding motion on the friction and wear of phenolic resin based composite," *Industrial Lubrication and Tribology*, vol. 71, no. 4, pp. 573–577, 2019.

[9] P. Xi, Q. Cong, S.-F. Ru, and B. Wu, "Wear resistance of piston skirt with bionic through hole," *Surface Technology*, vol. 47, pp. 86–92, 2018.

[10] A. Azzi, A. Maoui, A. Fatu, S. Fily, and D. Souchet, "Experimental study of friction in pneumatic seals," *Tribology International*, vol. 135, pp. 432–443, 2019.

[11] F. Hakami, A. Pramanik, N. Ridgway, and A. K. Basak, "Developments of rubber material wear in conveyer belt system," *Tribology International*, vol. 111, pp. 148–158, 2017.

[12] B. N. J. Persson, "Theory of powdery rubber wear," *Journal of Physics: Condensed Matter*, vol. 21, no. 48, Article ID 485001, 2009.

[13] S. F. Wu, D. R. Gao, Y. N. Liang, and B. Chen, "Experimental study on influence of dimples on lubrication performance of glass fiber-epoxy resin composite under natural seawater lubrication," *Chinese Journal of Mechanical Engineering*, vol. 30, no. 1, pp. 110–117, 2017.

[14] Y. J. Liu, D. Tang, J. Liu, and J. Lumkes, "Wear behaviour of piston seals in flow meter of fuel dispenser under different pressure conditions," *Flow Measurement and Instrumentation*, vol. 28, pp. 45–49, 2012.

[15] S. J. Zhang, W. C. Zhang, Y. B. Luo, and M. Chen, "Research on the method of detecting the failure of dynamic seal of direct-drive pump," *IOP Conference Series: Materials Science and Mechanical Engineering*, vol. 504, Article ID 012096, 2019.

[16] H. Zhang and J. Zhang, "Static and dynamic sealing performance analysis of rubber D-ring based on FEM," *Journal of Failure Analysis and Prevention*, vol. 16, no. 1, pp. 165–172, 2016.

[17] D. R. Gao, J. C. Liu, X. H. Xu, and Z. Y. Zhang, "Analysis on anti-wear mechanism of bionic non-smooth surface based on discrete phase model," *The Journal of Engineering*, vol. 2019, no. 13, pp. 32–36, 2019.

[18] S. Tsala, Y. Berthier, G. Mollon, and A. Bertinotti, "Numerical analysis of the contact pressure in a quasi-static elastomeric reciprocating sealing system," *Journal of Tribology*, vol. 140, no. 6, p. 7, 2018.

[19] Y. Q. Gu, T. X. Fan, J. G. Mou, L. F. Jiang, D. H. Wu, and S. H. Zheng, "A review of bionic technology for drag reduction based on analysis of abilities the earthworm," *International Journal of Engineering Research in Africa*, vol. 19, pp. 103–111, 2015.

[20] J. Q. Li, B. X. Kou, G. M. Liu, W. F. Fan, and L. L. Liu, "Resistance reduction by bionic coupling of the earthworm lubrication function," *Science China Technological Sciences*, vol. 53, no. 11, pp. 2989–2995, 2010.

[21] H. X. Zhao, Q. Q. Sun, X. Deng, and J. X. Cui, "Earthworm-inspired rough polymer coatings with self-replenishing lubrication for adaptive friction-reduction and antifouling surfaces," *Advanced Materials*, vol. 30, no. 29, Article ID 1802141, 2018.

[22] X. J. Cheng, T. Y. Gao, S. F. Ru, and Q. Cong, "Wear performance of bionic dimpled-shape pistons of mud pump," *Advances in Materials Science and Engineering*, vol. 2017, Article ID 8256429, 11 pages, 2017.